

1 **Carbonaceous Aerosols Recorded in a Southeastern Tibetan Glacier:**
2 **Analysis of Temporal Variations and Model Estimates of Sources**
3 **and Radiative Forcing**

4 Mo Wang^{1,2}, Baiqing Xu¹, Junji Cao³, Xuexi Tie^{3,4}, Hailong Wang², Rudong
5 Zhang^{5,2}, Yun Qian², Philip J. Rasch², Shuyu Zhao³, Guangjian Wu¹, Huabiao Zhao¹,
6 Daniel R. Joswiak¹, Jiule Li¹, Ying Xie¹

7 ¹*Key Laboratory of Tibetan Environment Changes and Land Surface Processes, Institute of*
8 *Tibetan Plateau Research, Chinese Academy of Sciences, Beijing 100101, China;*

9 ²*Atmospheric Sciences and Global Change Division, Pacific Northwest National Laboratory*
10 *(PNNL), Richland, WA 99352, USA;*

11 ³*State Key Laboratory of Loess and Quaternary Geology, Institute of Earth Environment,*
12 *Chinese Academy of Sciences, Beijing 100085, China;*

13 ⁴*National Center for Atmospheric Research, Boulder, CO, 80303, USA;*

14 ⁵*Key Laboratory for Semi-Arid Climate Change of the Ministry of Education, College of*
15 *Atmospheric Sciences, Lanzhou University, Lanzhou 730000, Gansu, China*

16 Corresponding author: Mo Wang

17 Email: wangmo@itpcas.ac.cn

18

19 **Abstract.** High temporal resolution measurements of black carbon (BC) and organic
20 carbon (OC) covering the time period of 1956-2006 in an ice core over the
21 southeastern Tibetan Plateau show a distinct seasonal dependence of BC and OC
22 with higher respective concentrations but lower OC/BC ratio in the non-monsoon
23 season than during the summer monsoon. We use a global aerosol-climate model, in
24 which BC emitted from different source regions can be explicitly tracked, to
25 quantify BC source-receptor relationships between four Asian source regions and
26 the southeastern Tibetan Plateau as a receptor. The model results show that South
27 Asia has the largest contribution to the present-day (1996-2005) mean BC
28 deposition at the ice core drilling site during the non-monsoon season (October to
29 May) (81%) and all year round (74%), followed by East Asia (14% to the
30 non-monsoon mean and 21% to the annual mean). The ice-core record also indicates
31 stable and relatively low BC and OC deposition fluxes from late 1950s to 1980,
32 followed by an overall increase to recent years. This trend is consistent with the BC
33 and OC emission inventories and the fuel consumption of South Asia (as the
34 primary contributor to annual mean BC deposition). Moreover, the increasing trend
35 of OC/BC ratio since the early 1990s indicates a growing contribution of coal
36 combustion and/or biomass burning to the emissions. The estimated radiative
37 forcing induced by BC and OC impurities in snow has increased since 1980,
38 suggesting an increasing potential influence of carbonaceous aerosols on the Tibetan
39 glacier melting and the availability of water resources in the surrounding regions.
40 Our study indicates that more attention to OC is merited because of its
41 non-negligible light absorption and the recent rapid increases evident in the ice core
42 record.

43 **Keywords**

44 Carbonaceous aerosol, Tibetan glacier, Emissions, Radiative forcing

45 **1. Introduction**

46 Carbonaceous aerosol, released from fossil fuel, biofuel and/or biomass
47 combustion, contains both black carbon (BC, a.k.a. elemental carbon, EC), a strong
48 light absorber, and organic carbon (OC), which also absorbs the near infrared, but
49 more weakly than BC (Kirchstetter et al., 2004; Bond et al., 2006). Often mixed
50 with other aerosol species, BC impacts human health, crop yields and regional
51 climate (Auffhammer et al., 2006; Tie et al., 2009), and is believed to be the second
52 strongest climate warming forcing agent after carbon dioxide (Jacobson, 2001; IPCC,
53 2013).

54 Because of their high population density and relatively low combustion
55 efficiency, developing countries in South and East Asia such as India and China are
56 hotspots of carbonaceous aerosol emissions (Ramanathan and Carmichael, 2008).
57 During the cold and dry winter season, haze (heavily loaded with carbonaceous
58 aerosols) builds up over South Asia, and exerts profound influences on regional
59 radiative forcing (Ramanathan et al., 2007; Ramanathan and Carmichael, 2008),
60 hydrologic cycles (Menon et al., 2002; Ramanathan et al., 2005), and likely
61 Himalaya-Tibetan glacier melting that could be accelerated by the absorption of
62 sunlight induced by BC in the air and deposited on the ice and snow surfaces
63 (Ramanathan et al., 2007; Hansen and Nazarenko, 2004), although BC deposited in
64 snow and glaciers at some locations may not significantly affect the energy balance
65 (Ming et al., 2013; Kaspari et al., 2014).

66 Due to the lack of long-term observations of emissions and concentrations of
67 atmospheric carbonaceous aerosols, it is difficult to evaluate the effects of BC and
68 OC on historical regional climate and environment before the satellite era. Some
69 studies have evaluated historical anthropogenic emissions based on the consumption
70 of fossil fuels and biofuels (Novakov et al., 2003; Ito and Penner, 2005; Bond et al.,
71 2007; Fernandes et al., 2007). While fossil fuel is the major energy source in the
72 urban areas of South Asia and East Asia, biomass combustion, such as fuel wood,
73 agricultural residue and dung cake, is prevalent in rural areas (Revelle, 1976;

74 Venkataraman et al., 2010; Street and Waldhoff, 1998). Biomass burning has been
75 considered as the major source of black carbon emissions (Reddy and Venkataraman,
76 2002; Venkataraman et al., 2005). However, as reliable biomass consumption data
77 are hard to obtain, estimates of BC and OC emissions from biomass burning are
78 ambiguous and incomplete.

79 Measurements of carbonaceous aerosol concentrations in glacier ice are an ideal
80 means to reconstruct historical emissions and reveal long-term trends of
81 anthropogenic aerosol impacts on local climate. Greenland ice core measurements
82 were previously used to reconstruct the North American BC emission history and its
83 effects on surface radiative forcing back to the 1880s (McConnell et al., 2007).
84 Himalayan ice cores retrieved from the Tibetan Plateau have revealed the mixed
85 historical emissions from South Asia, Central Asia and the Middle East and also
86 been used to evaluate radiative forcing from BC in snow (Ming et al., 2008; Kaspari
87 et al., 2011). Using the Snow, Ice, and Aerosol Radiative (SNICAR) model, Flanner
88 et al. (2007) estimated an instantaneous regional forcing of exceeding 20 W m^{-2} by
89 BC in snow/glaciers over the Tibetan Plateau during the spring season.

90 By using five ice core records, Xu et al. (2009a) elucidated an important
91 contribution of BC to the retreat of Tibetan glaciers in addition to greenhouse gases.
92 Due to the short atmospheric lifetime of carbonaceous aerosols compared to
93 greenhouse gases, emission reductions may be an effective way to mitigate their
94 warming effects. Thus it is particularly important to identify the source regions and
95 the source types of carbonaceous aerosols observed in Tibetan glaciers. Xu et al.
96 (2009a) suggested that BC deposited on Tibetan Plateau was broadly from Europe
97 and Asia. However, they didn't perform in-depth analysis on emissions from more
98 specific source regions and the source types. In this study, we use the ice core
99 retrieved from the southeastern Tibetan Plateau, also known as the Zuoqiupu ice
100 core in Xu et al. (2009a), to reconstruct the history of atmospheric deposition of
101 carbonaceous aerosols in this glacier, and to characterize emissions and

102 source-receptor relationships with the help of a global climate model in which BC
103 emitted from different source regions can be explicitly tracked. We also estimate the
104 respective contributions from BC and OC to radiative forcing in the Zuoqiupu
105 glacier using the ice core measurements and the SNICAR model.

106 **2. Methods**

107 **2.1 Measurements of carbonaceous aerosols in ice core**

108 Zuoqiupu glacier is in the southeastern Kangri Karpo Mountains, located at the
109 southeastern margin of the Tibetan Plateau (Figure 1). In 2007, an ice core of 97
110 meters in depth (9.5 cm in diameter) was retrieved within the accumulation zone of
111 Zuoqiupu glacier at 96.92°E, 29.21°N, 5600 m a.s.l. The ice core was kept frozen
112 and transported to laboratory facilities at the Institute of Tibetan Plateau Research
113 (Lhasa branch) for analysis. The annual accumulation of snow/ice at the drill site
114 was around 2 meters on average. The oxygen isotope ($\delta^{18}\text{O}$) samples were cut at 10
115 cm internals, and BC and OC samples at 10-25 cm, resulting in 18 and 9 samples per
116 year on average, respectively. Thus this ice core provided a high temporal-resolution
117 of $\delta^{18}\text{O}$, and BC and OC concentrations. BC and OC concentrations were measured
118 by using a Desert Research Institute (DRI) Model 2001 Thermal/Optical Carbon
119 Analyzer following the IMPROVE TOR protocol (Chow et al. 1993; Chow and
120 Watson 2002; Cao et al. 2008). Note that according to the thermal/optical
121 measurement method, the analytical result is technically called “EC”. Herein we use
122 “BC” to be consistent with the notation in our model simulations and in the literature.
123 The reported OC concentrations from the ice-core measurements can only account
124 for water-insoluble part of OC in the ice samples because most of the water-soluble
125 part cannot be captured by the filter-based method applied to liquid samples (melted
126 from the ice). Further details on the analysis methods, ice core dating and
127 calculation of BC and OC seasonal deposition fluxes can be found in Xu et al.

128 (2009a).

129 **2.2 Model and experimental setup**

130 We use the Community Atmosphere Model version 5 (CAM5; Neale et al.,
131 2012) to help understand the emissions, transport and dry/wet deposition of
132 carbonaceous aerosols in the atmosphere. In the default 3-mode modal aerosol
133 scheme of CAM5 used for this study, BC and primary OC are emitted into an
134 accumulation size mode, where they immediately mix with co-existing hygroscopic
135 species such as sulfate and sea salt (Liu et al., 2012). Hygroscopic aerosol particles
136 in the accumulation mode are subject to wet removal by precipitation. Recent model
137 improvements to the representation of aerosol transport and wet removal in CAM5
138 by Wang et al. (2013) have substantially improved the model prediction of global
139 distribution of aerosols, particularly, over remote regions away from major sources.
140 To minimize the model biases in simulating meteorological conditions and,
141 particularly, circulations that are critical to aerosol transport, we configure the
142 CAM5 model to run in an offline mode (Ma et al., 2013) with wind, temperature,
143 surface fluxes and pressure fields constrained by observations. However,
144 cloud/precipitation fields and interactions between aerosol and clouds are allowed to
145 evolve freely. A source tagging technique has been recently implemented in the
146 CAM5 model to allow for explicitly tracking aerosols emitted from individual
147 source regions and, therefore, assists in quantitatively characterizing source-receptor
148 relationships (Wang et al., 2014). This tagging technique along with the CAM5
149 model is used in the present study to do source attribution for carbonaceous aerosols
150 deposited to the Zuoqiupu glacier.

151 We conducted an 11-year (1995-2005) CAM5 simulation at horizontal grid
152 spacing of $1.9^\circ \times 2.5^\circ$ and 56 vertical levels, with prescribed sea surface
153 temperatures and sea ice distribution. Reanalysis products from NASA Modern Era
154 Retrospective-Analysis for Research and Applications (MERRA) (Rienecker et al.,

155 2011) are used to constrain the meteorological fields of CAM5. For aerosols
156 (including OC, BC and other important species), we use the year-2000 monthly
157 mean emissions described by Lamarque et al. (2010) that have been used in many
158 global climate models for present-day climate simulations, included in the fifth
159 assessment report (AR5) by the Intergovernmental Panel on Climate Change (IPCC).
160 The monthly mean emissions are repeatedly used for each year in the 11-year
161 simulation. Note that we do not intend to design the model experiment to simulate
162 the whole historical record of BC in the ice core, but rather for a period of time to
163 demonstrate the impact of meteorology (and associated transport and removal of
164 aerosols) on the seasonal dependence of BC deposition in the target region and the
165 lack of longer-term trend in deposition without considering the temporal variation of
166 emissions.

167 As the ice core drill site was located at a remote and elevated area over the
168 southeastern Tibetan Plateau, where local emissions are minimal. Deposition of
169 carbonaceous aerosols is most likely contributed by the non-local major emission
170 sources (e.g., distributions of mean BC emissions during non-monsoon and
171 monsoon seasons shown in Figure 2) in South Asia and East Asia. These two
172 regions, along with Southeast Asia and Central Asia, are identified as the potential
173 source contributors. Thus BC emissions from the four regions and the rest of the
174 world are explicitly tracked in the CAM5 simulation.

175 **3. Results and Discussion**

176 **3.1 Seasonal dependence of carbonaceous aerosols**

177 BC and OC concentrations in the Zuoqiupu ice core both exhibit statistically
178 significant seasonal variations at the 0.05 level corresponding to the stable oxygen
179 isotope variability, which shows high values during the winter and low values
180 during the summer (Xu et al., 2009a). As shown in Figure 3, concentrations of BC

181 and OC have distinct differences between the summer monsoon and non-monsoon
182 seasons. Seasonally varying emissions and meteorological conditions that determine
183 the transport pathways of BC and OC emitted from major sources, removal during
184 the transport, and local precipitation rate can cause the seasonal variations of BC and
185 OC in ice at the sampling site. The seasonal dependence of BC and OC in ice core is
186 consistent with available observations of atmospheric aerosols in the south slope of
187 the Himalayas and the southeastern Tibetan Plateau, where the high concentration of
188 carbonaceous aerosols during the cold and dry season was suggested to associate
189 with the South Asian haze (Cong et al., 2009; Marinoni et al., 2010; Kaspari et al.,
190 2011; Zhao et al., 2013a; Zhao et al., 2013b). The consistency between the seasonal
191 dependence of airborne BC and OC concentrations and the seasonal variation of
192 ice-core measurements indicates that seasonal differences in precipitation rate at the
193 sampling location is less likely to be the determining factor. Our model results
194 (details discussed in the section 3.2) suggest that the seasonal dependence of BC
195 deposition flux in the target region could be mainly due to meteorological conditions
196 that determine the transport pathways (and associated wet removal processes during
197 the transport). The small seasonal contrasts in BC emissions from the major source
198 regions (see Table 1) that are used in the model simulation do not seem to be able to
199 explain the large seasonal difference in BC deposition, although the BC emissions
200 are known to have large uncertainties.

201 Our further analysis shows that the ratio of OC to BC also has clear seasonal
202 dependence. In Figure 3, the slope of the fitted line to measured OC versus BC
203 concentrations during monsoon season is ~ 6.3 , which is twice the slope for
204 non-monsoon season (~ 3.2). The analysis of covariance (ANCOVA) for slope
205 differences of single linear regressions of OC against BC between monsoon and
206 non-monsoon seasons indicates that the seasonal dependence of the relationship
207 between the concentrations of OC and BC is significant (at the 0.05 significance
208 level). This also agrees with measurements derived from the ice core drilled from

209 the Palong-Zanbu No. 4 Glacier (Xu et al., 2009b) and in atmospheric samples
210 collected from Lulang, southeastern Tibetan Plateau (Zhao et al., 2013b). The
211 seasonal dependence of the OC/BC ratio can possibly be derived from the seasonal
212 sources of carbonaceous particles, circulation strength, transport pathways, and/or
213 atmospheric deposition processes. Compared to the respective BC and OC
214 concentrations, the seasonal dependence of OC/BC ratio is less straightforward to
215 understand. Circulation patterns together with wet removal processes still determine
216 the transport pathways of emissions from major BC and OC source regions to the
217 sampling site, which however are less likely to change OC/BC ratio from certain
218 sources. Therefore, it is more plausible due to seasonally dependent contributions
219 from source regions and/or emission sectors (including fuel types, quantity, and
220 combustion conditions). Cao et al. (2005) found that the average OC/BC ratios
221 measured from plumes of residential biomass burning and coal combustion are
222 substantially higher than from vehicle exhaust. Higher OC/BC ratio during summer
223 monsoon might indicate more contributions from biomass and/or coal burning than
224 fossil fuel combustion.

225 **3.2 Source attribution**

226 To quantitatively attribute the source of BC at the drilling site (as a receptor
227 region), we use the CAM5 model with the BC source tagging capability to conduct
228 an 11-year simulation, with the last 10 years (1996-2005) used for analysis. The
229 surrounding area is divided into four source regions (see Table 1 and Figure 4):
230 South Asia, East Asia, Southeast Asia and Central Asia. BC emissions from each of
231 the four regions and the rest of the world are explicitly tracked, so that the fractional
232 contributions by emissions from the individual source regions to BC deposition at
233 the receptor region can be explicitly calculated. Figure 4 shows the spatial
234 distribution of fractional contribution from the four source regions. BC deposition at
235 the drilling site (indicated by the black box in Figure 4), which has a consistent

236 seasonal dependence (i.e., more during the non-monsoon season; Figure 5) with ice
237 core measurements, is predominately (over 95%) from South Asia and East Asia.
238 The seasonal dependence of BC deposition is also consistent with a recent regional
239 climate modeling study on BC deposition on the Himalayan snow cover from 1998
240 to 2008 (Ménégoz et al., 2014).

241 The 10-year (1996-2005) average wind fields (at the surface and 500 hPa from
242 MERRA reanalysis datasets), as shown in Figure 2, indicate distinct circulation
243 patterns during summer monsoon (June-September) and non-monsoon
244 (October-May) season, which in part determine the seasonal dependence of transport
245 of aerosols emitted from the different major sources. During the non-monsoon
246 season, strong westerly dominates the transport from west to east at all levels.
247 Emissions from northern India and central Asia can have influence on BC in the
248 direct downwind receptor region over southeastern Tibetan Plateau. During the
249 summer monsoon season, the westerly moves northward and the monsoon flow from
250 Bay of Bengal at the surface and middle levels (e.g., 500hPa), coupled with the
251 monsoon from Indochina peninsula and South China Sea, exert influence on BC in
252 the receptor area. The strong monsoon precipitation removes BC from the
253 atmosphere during the transport. The high Himalayas can partly block the further
254 transport of emissions from South Asia to Tibetan Plateau, although small local
255 topographical features such as the Yarlung Tsangpo River valley can provide a gate
256 for the pollution to enter the inner Tibetan Plateau (Cao et al., 2010). Elevated
257 emissions from the west (or northern part of South Asia) can take the pathways at
258 middle and upper levels but they have minimal contribution to deposition. Therefore,
259 BC emissions from East Asia play a relatively more important role affecting
260 deposition at the Zuoqiupu site during the monsoon season.

261 The fractional contributions to 10-year mean BC deposition at the drilling site
262 from the four tagged regions are summarized in Table 1. Results show that South
263 Asia is the dominant contributor (~81%) during the non-monsoon season with ~14%

264 from East Asia, while the contribution of East Asia (~56%) is larger than that of
265 South Asia (~39%) during the monsoon season. For the annual mean BC deposition,
266 South Asia (~75%) is the biggest contributor, followed by East Asia (~21%).
267 Emissions from the central Asia and Southeast Asia regions have much smaller
268 contributions (<3%) for all seasons. These results agree well with the short-term
269 source attribution study by Lu et al. (2012) using the Hybrid Single-Particle
270 Lagrangian Integrated Trajectory (HYSPLIT) model.

271 For comparison, seasonal and annual mean BC emissions from the individual
272 tagged source regions are also included in Table 1. Apparently, the contrast in
273 strengths of regional emissions alone cannot explain their relative contributions to
274 BC deposition at the sampling site, and the small seasonal variations in emissions
275 are unlikely the cause of seasonal dependence of source attribution. Note that the BC
276 emission inventory (Lamarque et al., 2010) used in CAM5 doesn't consider seasonal
277 variations in anthropogenic emissions, which is likely to have introduced biases in
278 the quantitative model estimates of seasonal dependence of contributions, but the
279 relative importance of source regions should be robust.

280 **3.3 Interannual variations and long-term trend**

281 Based on annual snow accumulation and BC and OC concentrations derived
282 from the ice record, the annual BC and OC deposition fluxes can be estimated,
283 which are then used to examine the interannual variations and long-term trend in the
284 fluxes and the ratio of OC/BC, as well as the relationship with emissions from the
285 major contributor. As illustrated in Figure 6, from late 1950s to 1980, the BC and
286 OC fluxes in the Zuoqiupu ice core are relatively low and stable in comparison to
287 those after 1980. During the period 1956 to 1979, average fluxes are 9.1 and 28.7
288 $\text{mg m}^{-2} \text{ a}^{-1}$ for BC and OC, respectively. Both BC and OC fluxes began to show
289 increasing trends from early 1980s. These trends continued in the early 1990s but
290 started to drop in the mid-1990s, reaching a minimum in 2002 followed by a rapid

291 increase. In 2006, BC and OC fluxes are 19.2 and $93.9 \text{ mg m}^{-2} \text{ a}^{-1}$, respectively,
292 which are two and three times the respective average fluxes before 1980. The
293 five-year average OC/BC flux ratio is steady before 1990; however, it shows a
294 continual increase afterwards and has been higher than the average value (3.2) for
295 the period of 1956-1979 since mid-1990s (Figure 6). The 10-year CAM5 model
296 simulation, in which annual emissions are fixed but meteorological conditions vary,
297 shows no increasing trend in BC and OC deposition fluxes (BC deposition shown in
298 Figure 5), indicating that the increasing trend seen in the observations was not due to
299 changes in meteorology.

300 As shown in the CAM5 model simulation, the annual mean atmospheric
301 deposition of BC over southeastern Tibetan Plateau is mostly contributed by
302 emissions from South Asia, particularly, in the non-monsoon season. The BC and
303 OC deposition fluxes derived from the ice-core measurements may reflect changes
304 in South Asian emissions to some extent. The temporal variations of BC and OC
305 deposition fluxes (see Figure 6) are compared with the primary BC and OC
306 emissions from fossil fuel and biofuel combustion in South Asia during 1955-2000
307 (Bond et al., 2007). BC and OC emissions during 1996-2010 from Lu et al. (2011)
308 are also illustrated in Figure 6 to extend the emission data to cover the entire time
309 period that the ice core data span. Note that the emission data from Lu et al. (2011)
310 are only for India, which is the largest energy consumer and carbonaceous
311 aerosol-emitting country in South Asia. There are differences between the emissions
312 of Bond et al. and Lu et al. during the overlap time period (1996-2000). However,
313 good agreements on the increasing trend can be found in the respective deposition
314 fluxes and emissions of BC and OC (Figure 6). The OC/BC emission ratio also
315 shows an increasing trend from the late 1990s to 2003, which is consistent with that
316 of OC/BC ratio in the ice core record. The annual mean aerosol index over industrial
317 and populated cities in the northern part of India increased from 1982-1993 and
318 more significantly from 2000-2003 (Sarka et al., 2006). This trend is similar to that

319 of carbonaceous aerosols in the ice core record, and it might indicate a causal
320 relationship between BC and OC over southeastern Tibetan Plateau and emissions
321 from north part of South Asia.

322 **3.4 Emission source analyses**

323 BC and OC in the atmosphere are co-emitted from a variety of natural and
324 anthropogenic sources, including combustion of fossil fuel, biofuel and/or biomass
325 burning. In general, open biomass burning typically produces more abundant OC
326 (i.e., larger OC/BC ratio) compared to fossil fuel combustion due to a lower process
327 temperature (Ducret and Cachier, 1992). The OC/BC ratio has often been used to
328 discriminate fossil fuel combustion and biomass burning emissions in the
329 atmosphere and in precipitation (Novakov et al., 2000; Stone et al., 2007; Ducret
330 and Cachier, 1992; Xu et al., 2009b). For example, Cao et al. (2005) collected
331 particulate matter samples from the plumes of residential biomass burning, coal
332 combustion, and motor-vehicle exhaust sources, and analyzed OC and BC with DRI
333 Thermal/Optical Carbon Analyzer (Model 2001). They reported average OC/BC
334 ratios of 60.3, 12.0, and 4.1 for biomass burning, coal-combustion and vehicle
335 exhaust, respectively. The increasing OC/BC ratios based on the ice core
336 measurements since the early 1990s (Figure 6) suggest an expanded coal
337 consumption and/or usage of biomass fuel, although the ratios might have been
338 underestimated because water-soluble OC was not captured in the sample analyses.
339 However, such bias would have occurred to all the samples and had little impact on
340 the trend, unless including water-soluble OC could dominate the temporal variation
341 of OC/BC ratio. Otherwise, our results indicate that the relative contribution of coal
342 combustion and biomass burning to the carbonaceous particles deposited into the ice
343 core in southeastern Tibetan Plateau has been increasing faster than the contribution
344 of fossil fuel combustion since early 1990s. Improved combustion technologies may
345 have reduced both BC and OC emissions from the combustion of the same amount

346 of fuels, but the influence on OC/BC ratio is unclear. Presumably improved
347 combustion technologies after 1990 in South and East Asia did not dominate the
348 OC/BC ratio.

349 The temporal variations of BC and OC in the Zuoqiupu ice core, along with the
350 source attribution analysis of the CAM5 model results, suggest an increasing trend
351 in emissions and altered emission sources in South Asia during the late 20th century.
352 Coal has been the primary energy source in South Asia. For example, in India coal
353 accounted for 41% of the total primary energy demand in 2007, followed by
354 biomass (27%) and oil (24%) (IEA, 2009). The consumption data of coal and crude
355 oil in South Asia (BP Group, 2009) is compared with the BC and OC fluxes in
356 Figure 6 (bottom right). Coal consumption had an increasing trend from 1965 to
357 2008, particularly in the two time periods 1980-1995 and 2003-2008 after a level off
358 during 1996-2002. This trend is consistent with the variations of BC and OC
359 deposition fluxes in the Zuoqiupu ice core. The correlations between coal
360 consumption and BC ($R^2 = 0.43$, $p < 0.001$) and OC ($R^2 = 0.62$, $p < 0.001$) in the ice
361 core are both statistically significant. The oil consumption had a comparable
362 increasing trend as coal before it slowed down during 2000-2006.

363 Biomass is the second largest energy resource in South Asia, and it is essential
364 in rural areas. In India, 70% of the population lives in rural areas, and depends
365 substantially on solid fuels (i.e., firewood, animal dung, and agriculture residues) for
366 cooking and heating (Heltberg et al., 2000). Even in urban areas, biomass
367 contributes to 27% of the household cooking fuel (Venkataraman et al., 2010).
368 Although the consumption of biomass is lower than coal, the OC/BC emission ratio
369 for biomass burning is much higher than from coal combustion (60.3 vs. 12.0) (Cao
370 et al., 2005). BC emission factor for biomass burning (varying from 0.48 ± 0.18 g
371 kg^{-1} for savanna and grassland burning to 1.5 g kg^{-1} for charcoal burning) is also
372 generally higher than that for coal (0.2 g kg^{-1} for most combustion conditions) and
373 oil combustion (0.3 g kg^{-1} on average, varying from 0.08 g kg^{-1} for heavy fuel oil to

374 0.66 g kg⁻¹ for diesel) (Andreae and Merlet, 2001; Bond et al., 2004, 2007).
375 Therefore, it is very likely that the OC/BC ratio of atmospheric carbonaceous
376 aerosols and in the ice-core samples (Figure 6) was dominated by biomass burning
377 emissions. Previous studies have concluded that carbonaceous aerosol emissions
378 from biomass burning are the largest source in South Asia (Venkataraman et al.,
379 2005; Gustafsson et al., 2009). A general increase in energy-intensive life-styles
380 associated with the accelerated growth of population and economy put pressure on
381 energy resources, and induced energy transitions and use of non-sustainable biomass
382 in South Asia (Sathaye and Tyler, 1991; Pachauri, 2004; Fernandes et al., 2007). For
383 instance, biofuel consumption in South Asia increased by 21% per decade on
384 average during 1950-2000 (Bond et al., 2007; Fernandes et al., 2007). In addition,
385 fuel wood, a more desirable biofuel option, contributed 68% in 1978 to total energy
386 demand by rural populations in India, and increased to 78% in 2000 (Fernandes et
387 al., 2007).

388 **3.5 Radiative forcing induced by carbonaceous aerosols in Tibetan Glaciers**

389 BC is often the most important light-absorbing impurity in surface snow
390 because of its strong absorption of solar radiation. Effect of BC in snow on surface
391 albedo reduction and resultant positive radiative forcing have been widely addressed
392 and reported (e.g., Warren and Wiscombe, 1980; Clarke and Noone, 1985; Hansen
393 and Nazarenko, 2004; Hadley and Kirchstetter, 2012; Flanner et al., 2007; 2009;
394 McConnell et al., 2007; Ming et al., 2008; Kaspari et al., 2011; Qian et al., 2011,
395 2014, 2015). In contrast, the impact of OC in snow has not been widely assessed
396 because of its relatively weak light-absorption over the entire spectrum compared to
397 BC, and because of large uncertainties associated with OC light-absorbing
398 properties and measurements of OC in snow. However, there have been increasing
399 interests in light-absorbing OC (a.k.a. brown carbon) and its radiative effect in both
400 the atmosphere and snow. A growing number of studies (e.g., Kirchstetter et al.,

401 2004; Andreae and Gelencsér, 2006; Hoffer et al., 2006; Yang et al., 2009;
402 Kirchstette and Thatcher, 2012) have reported that airborne brown carbon can
403 contribute significantly to aerosol light absorption in the atmosphere, although there
404 are still substantial uncertainties in quantifying optical properties of brown carbon,
405 which makes the model estimation of OC radiative forcing difficult. Similarly, the
406 importance of OC absorption in snow has been recognized and suggested for
407 inclusion in modeling aerosol snow-albedo effect (e.g., Flanner et al., 2009; Aoki et
408 al., 2011). Observational analysis of light-absorbing particles in Arctic snow
409 reported that the main non-BC component is brown carbon, which accounted for
410 20-50% of the visible and ultraviolet absorption (Hegg et al., 2009, 2010; Doherty et
411 al., 2010). In the rural area of central north China, brown carbon in winter snow also
412 played an important role in visible light absorption, which contributed about 60% to
413 light absorption at 450 nm and about 40% at 600 nm (Wang et al., 2013). A more
414 recent observational study by Dang and Hegg (2014) qualified the light absorption
415 by different light-absorbing particulates in snow, and suggested that humic-like
416 substances and polar OC contributed 9% and 4% to the total light absorption
417 respectively. Despite the substantial uncertainties in brown carbon optical properties,
418 a recent global modeling study (Lin et al., 2014), in which a range of optical
419 properties of brown carbon taken from the literature were applied to OC-in-snow
420 concentrations simulated in a global chemical transport model, showed that the
421 global OC forcing in land snow and sea ice is up to 24% of that caused by BC. Thus
422 the contribution of OC in snow to the surface albedo reduction is likely to be
423 important, which has also been considered in recent climate modeling studies (Qian
424 et al., 2015).

425 In this study, we use the SNICAR-online model (available at
426 <http://snow.engin.umich.edu/>; Flanner et al., 2007) to estimate radiative forcing
427 induced by the observed BC as if they were present in snow. Detailed description of
428 the SNICAR model has been documented by Flanner and Zender (2005, 2006) and

429 Flanner et al. (2007). Here we only briefly describe the setup of input parameters
430 required for running the SNICAR model. A mass absorption cross-section (MAC) of
431 $7.5 \text{ m}^2 \text{ g}^{-1}$ at 550 nm for uncoated BC particle (Bond and Bergstrom, 2006) is
432 assumed to be same as the default value, and thus one of the input parameters for
433 adjusting the MAC value in the online SNICAR model, MAC scaling factor, is set to
434 1. According to the previous studies (Cuffey and Paterson, 2010; Wiscombe and
435 Warren 1980) and measurements in Qiyi glacier and Zuoqiupu glacier, an effective
436 radius of $100 \text{ }\mu\text{m}$ with density of 60 kg m^{-3} for new snow, and the effective radius of
437 $400 \text{ }\mu\text{m}$ with density of 400 kg m^{-3} for aged snow are adopted for the forcing
438 calculation. As we focus on the estimation of radiative forcing by carbonaceous
439 particles, other impurity contents, such as dust and volcanic ash, are set to be zero.
440 The annual mean BC concentration during 1956-1979 was 4.4 ng g^{-1} , and increased
441 to 12.5 ng g^{-1} in 2006. As a consequence, the annual mean radiative forcing induced
442 by BC in snow, as calculated by the SNICAR model, nearly proportionally increases
443 from 0.75 W m^{-2} to 1.95 W m^{-2} . Our estimate of mean BC forcing is lower than the
444 estimated Eurasian radiative forcing (2.7 W m^{-2}) in spring (Flanner et al., 2009), but
445 it's comparable to that in the East Rongbuk glacier over Himalayas, which was in
446 the range of $1\text{-}2 \text{ W m}^{-2}$ (Ming et al., 2008). Kaspari et al. (2009) reported a
447 three-fold increase in radiative forcing from BC in snow over Himalayas after 1975,
448 which is consistent with the increasing trend in our results.

449 The SNICAR model currently does not support the calculation of OC-in-snow
450 forcing in the same way as that for BC due to a lack of reliable OC optical properties
451 that span the dimensions of snow grain size and OC particle size (personal
452 communication with Mark Flanner, 2014). We take a MAC value of $0.6 \text{ m}^2 \text{ g}^{-1}$ at
453 550 nm for OC (Kirchstetter et al., 2004), and assume a constant factor of 0.08 (i.e.,
454 $0.6/7.5$) to scale down MAC values of BC at all wavelengths to obtain a first-order
455 guess of OC-in-snow forcing using SNICAR. The estimated OC forcing has a 4-fold
456 increase from 0.2 W m^{-2} (for mean OC concentration of 13.8 ng g^{-1} during

457 1956-1979) to 0.84 W m^{-2} (for mean OC concentration of 61.3 ng g^{-1} in 2006),
458 which are 27% and 43% of corresponding BC-in-snow forcing, respectively. The
459 BC/OC forcing ratios based on our simple guesses are larger than the upper bound
460 of estimates (i.e., 24%) by Lin et al. (2014).

461 Two main assumptions could have caused our first-order estimate of OC
462 forcing to have large biases. First, the MAC value of $0.6 \text{ m}^2 \text{ g}^{-1}$ (at 550 nm) was
463 based on OC extracted from biomass burning samples that tends to have higher
464 absorption efficiency than OC emitted from fossil fuel combustion (Kirchstetter et al.,
465 2004). This may cause an overestimation of OC forcing. Second, we treated all the
466 water-insoluble OC from the ice-core measurements as light-absorbing brown
467 carbon in the forcing estimation, which also likely results in an overestimation of
468 OC forcing if a significant fraction of OC is non-absorbing. However, water-soluble
469 part, accounting for about half of OC observed in Manora peak and northwest India
470 (Ram et al., 2010; Rajput et al., 2013), can also contribute to some absorption of UV
471 and visible light (Chen and Bond, 2010; Beine et al., 2011). Thus the absorption by
472 water-soluble OC that was not included in the forcing estimate may compensate for
473 the high bias to some extent. According to a laboratory study by Chen and Bond
474 (2010), a large fraction of absorbing OC from hard wood burning is water-insoluble.
475 As water-insoluble OC recorded in the ice core herein was very likely dominated by
476 biomass burning emissions (Section 3.4), the second assumption we used here may
477 not cause a huge bias in estimating OC forcing in snow.

478 It is also important to note that we didn't consider variations in chemical
479 compounds of OC, the changes of OC during sample filtration, and the different
480 spectral dependence of OC and BC absorption. Although such uncertainties can also
481 cause bias in the estimation of OC radiative forcing herein, the increasing trend
482 should be robust.

483 BC and OC concentrations in the ice core increased rapidly since 1980, and the

484 induced radiative forcing rose as a consequence. According to the estimates using
485 the SNICAR model, the average BC radiative forcing had increased 43% after 1980,
486 and OC radiative forcing had an increase of 70%. These numbers are by no means
487 accurate, but the stronger increasing trend in the ice core recorded OC than BC
488 during 1990-2006 (Figure 6) suggests that the contribution of OC to the total
489 radiative forcing in the glacier induced by snow/ice impurities deserves more
490 attention.

491 **4. Summary and Conclusions**

492 Light-absorbing carbonaceous aerosols can induce significant warming in the
493 atmosphere and in snow and glaciers, which likely accelerates the melting of
494 glaciers over Himalayas and Tibetan Plateau. Ice-core measurement of carbonaceous
495 aerosols is a useful mechanism for evaluating historical emission inventories and
496 revealing long-term changes in anthropogenic aerosols and their impacts on regional
497 climate. In this study, we analyze carbonaceous aerosols recorded in an ice core (97
498 meters in depth and 9.5 cm in diameter) retrieved from the Zuoqiupu glacier
499 (96.92°E, 29.21°N, 5600 m above sea level) in the southeastern Tibetan Plateau for
500 their seasonal dependence and long-term trend. The glacier has a unique
501 geographical location that is in close proximity to major Asian emission sources.
502 With the help of a global climate model (CAM5) in which black carbon (BC)
503 emitted from different source regions can be explicitly tracked, we are able to
504 characterize BC source-receptor relationships between four Asian source regions
505 (i.e., South Asia, East Asia, Southeast Asia and Central Asia) and the Zuoqiupu
506 glacier area as a receptor. We also estimate the radiative forcing in snow due to BC
507 and OC using the ice core measurements and an offline snow-ice-aerosol-radiation
508 model (called SNICAR).

509 BC and OC concentrations in small segments of the Zuoqiupu ice core were
510 measured using a thermal-optical method. Ice core dating based on significant

511 seasonal variations of oxygen isotope ratios ($\delta^{18}\text{O}$) was used to construct the time
512 series of BC and OC concentrations, which turned out to span the time period of
513 1956–2006. Not only do the concentrations of OC and BC in the ice core exhibit
514 significant differences between the summer monsoon and non-monsoon seasons,
515 which is likely due to changes in transport pathways and wet removal, but also the
516 ratio of OC to BC shows a clear seasonal dependence that might be due to seasonal
517 change in contributions from source regions and/or emission sectors. The CAM5
518 results show a similar seasonal dependence of BC and OC deposition to the glacier.

519 The MERRA reanalysis products used to drive the CAM5 model simulation
520 show distinct circulation patterns during summer monsoon (June-September) and
521 non-monsoon (October-May) seasons. Both the circulation patterns (and associated
522 aerosol transport and wet removal) and seasonal variation of emissions in major
523 source regions influence the seasonal deposition of aerosol at the Zuoqiupu site. The
524 CAM5 simulation with tagged BC regional sources shows that South Asia is the
525 dominant contributor (81%) to the 10-year mean BC deposition at the Zuoqiupu site
526 during the non-monsoon season with 14% from East Asia, while the contribution of
527 East Asia (56%) is larger than that of South Asia (39%) during the monsoon season.
528 For the annual mean BC deposition, South Asia (75%) is the biggest contributor,
529 followed by East Asia (21%).

530 The annual mean BC and OC deposition fluxes into the ice core are also
531 estimated to explore the interannual variations and long-term trends. Results show
532 stable and relatively low BC and OC fluxes from late 1950s to 1979, followed by a
533 steady increase through the mid-1990s. A more rapid increase occurred after the
534 minimum in 2002. The BC and OC deposition fluxes in 2006 were two and three
535 times the respective average before 1980.

536 The overall increasing trend in deposition fluxes since 1980 is consistent with
537 the BC and OC emissions in South Asia as the major contributor. Moreover, the
538 increasing trend of OC/BC ratio since early 1990s indicates a growth of the

539 contribution of coal combustion and/or biomass burning to the carbonaceous aerosol
540 emissions in the major contributing source regions, which is consistent with the
541 trends in the consumption of coal, oil and biomass in South Asia.

542 Our offline calculation using the SNICAR model shows a significant increase of
543 radiative forcing induced by the observed BC and OC in snow after 1980, which has
544 implications for the Tibetan glacier melting and availability of water resources in the
545 surrounding regions. More attention to OC is merited because of its non-negligible
546 light absorption and the recent rapid increases evident in the ice core record.

547

548 **Acknowledgements**

549 This work was supported by the China National Funds for Distinguished Young
550 Scientists and the National Natural Science Foundation of China, including
551 41125003, 41101063, 2009CB723901. H. Wang, Y. Qian and P.J. Rasch were
552 supported by the U.S. Department of Energy (DOE), Office of Science, Biological
553 and Environmental Research as part of the Earth System Modeling program. R.
554 Zhang acknowledges support from the China Scholarship Fund. PNNL is operated
555 for DOE by Battelle Memorial Institute under contract DE-AC05-76RLO1830. The
556 National Center for Atmospheric Research is sponsored by the National Science
557 Foundation. We thank Zhongming Guo and Song Yang for providing the
558 observations of snow.

559 **References**

- 560 Andreae, M. O. and Gelencsér, A.: Black carbon or brown carbon? The nature of
561 light-absorbing carbonaceous aerosols, *Atmos. Chem. Phys.*, 6, 3131-3148,
562 doi:10.5194/acp-6-3131-2006, 2006.
- 563 Andreae, M. O., and Merlet, P.: Emission of trace gases and aerosols from biomass
564 burning, *Global Biogeochem. Cy.*, 15, 955-966, doi: 10.1029/2000GB001382, 2001.
- 565 Aoki, T., Kuchiki, K., Niwano, M., Kodama, Y., Hosaka, M., and Tanaka T.:
566 Physically based snow albedo model for calculating broadband albedos and the solar
567 heating profile in snowpack for general circulation models, *J. Geophys. Res.*, 116,
568 D11114, doi: 10.1029/2010JD015507, 2011.
- 569 Auffhammer, M., Ramanathan, V., and Vincent, J. R.: Integrated model shows that
570 atmospheric brown clouds and greenhouse gases have reduced rice harvests in India,
571 *Proc. Natl. Acad. Sci. USA*, 103, 19668–19672, 2006.
- 572 Beine, H., Anastasio, C., Esposito, G., Patten, K., Wilkening, E., Domine, F., Voisin,
573 D., Barret, M., Houdier, S., and Hall S.: Soluble, light-absorbing species in snow at
574 Barrow, Alaska, *J. Geophys. Res.*, 116, D00R05, doi:10.1029/2011JD016181, 2011.
- 575 Bond, T. C. and Bergstrom, R. W.: Light absorption by carbonaceous particles: an
576 investigative review, *Aerosol. Sci. Tech.*, 40, 27–67, 2006.
- 577 Bond, T. C., Bhardwaj, E., Dong, R., Jogani, R., Jung, S., Roden, C., Street, D. G.,
578 and Trautmann, N. M.: Historical emissions of black and organic carbon aerosol from
579 energy-related combustion, 1850–2000, *Global Biogeochem. Cy.*, 21, GB2018,
580 doi:10.1029/2006GB002840, 2007.
- 581 BP Group: BP Statistical Review of World Energy June 2009, Report, BP p.l.c.,
582 London, UK, 45 pp., 2009.
- 583 Cao, J. J., Wu, F., Chow, J. C., Lee, S. C., Li, Y., Chen, S. W., An, Z. S., Fung, K. K.,
584 Watson, J. G., Zhu, C. S., and Liu, S. X.: Characterization and source apportionment
585 of atmospheric organic and elemental carbon during fall and winter of 2003 in Xi'an,
586 China, *Atmos. Chem. Phys.*, 5, 3127–3137, doi:10.5194/acp-5-3127-2005, 2005.
- 587 Cao, J., Tie, X., Xu, B., Zhao, Z., Zhu, C., Li, G., and Liu, S.: Measuring and
588 modeling black carbon (BC) contamination in the SE Tibetan Plateau, *J. Atmos.*
589 *Chem.*, 67, 45–60, 2010.
- 590 Cao, J., Zhu, C., Chow, J., Liu, W., Han, Y., and Watson, J. G.: Stable carbon and
591 oxygen isotopic composition of carbonate in fugitive dust in the Chinese Loess
592 Plateau, *Atmos. Environ.*, 42, 9118–9122, 2008.

593 Chen, Y. and Bond, T. C.: Light absorption by organic carbon from wood combustion,
594 *Atmos. Chem. Phys.*, 10, 1773-1787, doi:10.5194/acp-10-1773-2010, 2010.

595 Chow, J. C. and Watson, J. G.: PM_{2.5} carbonate concentrations at regionally
596 representative interagency monitoring of protected visual environment sites, *J.*
597 *Geophys. Res.*, 107, 8344, doi:10.1029/2001JD000574, 2002.

598 Chow, J. C., Watson, J. G., Pritchett, L. C., Pierson, W. R., Frazier, C. A., and Purcell,
599 R. G.: The DRI thermal/optical reflectance carbon analysis system: description,
600 evaluation and applications in US air quality studies, *Atmos. Environ.*, 27, 1185–1201,
601 1993.

602 Clarke, A. D. and Noone, K. J.: Soot in the Arctic snowpack: a cause for perturbations
603 in radiative transfer, *Atmos. Environ.*, 19, 2045–2053, 1985.

604 Cong, Z., Kang, S., and Qin, D.: Seasonal features of aerosol particles recorded in
605 snow from Mt. Qomolangma (Everest) and their environmental implications, *J.*
606 *Environ. Sci.*, 21, 914–919, 2009.

607 Cuffey, K. M. and Paterson, W. S. B. (Eds.): *The physics of glaciers*, Fourth Edition,
608 Academic Press, Burlington, USA, 2010.

609 Dang, C., and Hegg, D. A.: Quantifying light absorption by organic carbon in
610 Western North American snow by serial chemical extractions, *J. Geophys. Res.*
611 *Atmos.*, 119, 10,247–10,261, doi:10.1002/2014JD022156, 2014.

612 Doherty, S. J., Grenfell, T. C., Forsström, S., Hegg, D. L., Brandt, R. E., and Warren,
613 S. G.: Observed vertical redistribution of black carbon and other insoluble
614 light-absorbing particles in melting snow, *J. Geophys. Res. Atmos.*, 118, 5553–5569,
615 doi:10.1002/jgrd.50235, 2013.

616 Ducret, J. and Cachier, H.: Particulate carbon content in rain at various temperate and
617 tropical locations, *J. Atmos. Chem.*, 15, 55–67, 1992.

618 Fernandes, S. D., Trautmann, N. M., Streets, D. G., Roden, C. A., and Bond, T. C.:
619 Global biofuel use, 1850–2000, *Global Biogeochem. Cy.*, 21, GB2019,
620 doi:10.1029/2006GB002836, 2007.

621 Flanner, M. G. and Zender, C. S.: Linking snowpack microphysics and albedo
622 evolution, *J. Geophys. Res.*, 111, D12208, doi:10.1029/2005JD006834, 2006.

623 Flanner, M. G. and Zender, C. S.: Snowpack radiative heating: influence on Tibetan
624 Plateau climate, *Geophys. Res. Lett.*, 32, L06501, doi:10.1029/2004GL022076, 2005.

625 Flanner, M. G., Zender, C. S., Hess, P. G., Mahowald, N. M., Painter, T. H.,
626 Ramanathan, V., and Rasch, P. J.: Springtime warming and reduced snow cover from

627 carbonaceous particles, *Atmos. Chem. Phys.*, 9, 2481-2497,
628 doi:10.5194/acp-9-2481-2009, 2009.

629 Flanner, M. G., Zender, C. S., Randerson, J. T., and Rasch, P. J.: Present-day climate
630 forcing and response from black carbon in snow, *J. Geophys. Res.*, 112, D11202,
631 doi:10.1029/2006JD008003, 2007.

632 Gustafsson, Ö, Kruså, M., Zencak, Z., Sheesley, R. J., Granat, L., Engström, E.,
633 Praveen, P. S., Rao, P. S. P., Leck, C., and Rodhe, H.: Brown clouds over South Asia:
634 Biomass or fossil fuel combustion?, *Science*, 323, 495–497, 2009.

635 Hadley, O. L. and Kirchstetter, T. W.: Black-carbon reduction of snow albedo, *Nat.*
636 *Clim. Change*, 2, 437–440, 2012.

637 Hansen, J. and Nazarenko, L.: Soot climate forcing via snow and ice albedos, *Proc.*
638 *Natl. Acad. Sci. USA*, 101, 423–428, 2004.

639 Hegg, D. A., Warren, S. G., Grenfell, T. C., Doherty, S. J., Larson, T. V., and Clarke,
640 A. D.: Source attribution of black carbon in snow, *Env. Sci. Tech.*, 43(11), 4016–4021,
641 doi: 10.1021/es803623f, 2009.

642 Hegg, Dean A., Warren, Stephen G., Grenfell, Thomas C., Sarah J Doherty, and
643 Clarke, Antony D.: Sources of light-absorbing aerosol in arctic snow and their
644 seasonal variation, *Atmos. Chem. Phys.*, 10, 10923-10938,
645 doi:10.5194/acp-10-10923-2010, 2010.

646 Heltberg, R., Arndt, T. C., and Sekhar, N. U.: Fuelwood consumption and forest
647 degradation: a household model for domestic energy consumption in rural India, *Land*
648 *Econ.*, 76, 213–232, 2000.

649 Hoffer, A., Gelencsér, A., Guyon, P., Kiss, G., Schmid, O., Frank, G. P., Artaxo, P.,
650 and Andreae, M. O.: Optical properties of humic-like substances (HULIS) in
651 biomass-burning aerosols, *Atmos. Chem. Phys.*, 6, 3563-3570,
652 doi:10.5194/acp-6-3563-2006, 2006.

653 IEA: Chapter 9 – Country and regional profiles in the 450 Scenario, in: *World Energy*
654 *Outlook 2009*, International Energy Agency, France, 319–362, 2009.

655 IPCC: *Climate Change 2013: The Physical Science Basis*, Contribution of Working
656 Group I to the Fourth Assessment Report of the Intergovernmental Panel on Climate
657 Change, edited by Solomon, S., D. Qin, M. Manning, Z. Chen, M. Marquis, K.B.
658 Averyt, M. Tignor and H.L. Miller, Cambridge University Press, Cambridge, United
659 Kingdom and New York, NY, USA, 996 pp., 2013.

660 Ito, A. and Penner, J. E.: Historical emissions of carbonaceous aerosols from biomass

661 and fossil fuel burning for the period 1870–2000, *Global Biogeochem. Cy.*, 19,
662 GB2028, doi:10.1029/2004GB002374, 2005.

663 Jacobson, M. Z.: Strong radiative heating due to the mixing state of black carbon in
664 atmospheric aerosols, *Nature*, 409, 695–697, 2001.

665 Kaspari, S. D., Schwikowski, M., Gysel, M., Flanner, M. G., Kang, S., Hou, S., and
666 Mayewski, P. A.: Resent increase in black carbon concentrations from a Mt. Everest
667 ice core spanning 1860–2000 AD, *Geophys. Res. Lett.*, 38, L04703,
668 doi:10.1029/2010GL046096, 2011.

669 Kaspari, S., Painter, T. H., Gysel, M., Skiles, S. M., and Schwikowski, M.: Seasonal
670 and elevational variations of black carbon and dust in snow and ice in the
671 Solu-Khumbu, Nepal and estimated radiative forcings, *Atmos. Chem. Phys.*, 14,
672 8089-8103, doi:10.5194/acp-14-8089-2014, 2014.

673 Kirchstetter, T. W. and Thatcher, T. L.: Contribution of organic carbon to wood
674 smoke particulate matter absorption of solar radiation, *Atmos. Chem. Phys.*, 12,
675 6067-6072, doi:10.5194/acp-12-6067-2012, 2012.

676 Kirchstetter, Thomas W., Novakov, T., and Hobbs, Peter V.: Evidence that the
677 spectral dependence of light absorption by aerosol is affected by organic carbon, *J.*
678 *Geophys. Res.*, 109, D21208, doi:10.1029/2004JD004999, 2004.

679 Lamarque, J.-F., Bond, T. C., Eyring, V., Granier, C., Heil, A., Klimont, Z., Lee, D.,
680 Liou, C., Mieville, A., Owen, B., Schultz, M. G., Shindell, D., Smith, S. J.,
681 Stehfest, E., Van Aardenne, J., Cooper, O. R., Kainuma, M., Mahowald, N.,
682 McConnell, J. R., Naik, V., Riahi, K., and van Vuuren, D. P.: Historical (1850–2000)
683 gridded anthropogenic and biomass burn ing emissions of reactive gases and aerosols:
684 methodology and application, *Atmos. Chem. Phys.*, 10, 7017–7039,
685 doi:10.5194/acp-10-7017-2010, 2010.

686 Lin, G., Penner, J. E., Flanner, M. G., Sillman, S., Xu, L., and Zhou, C.: Radiative
687 forcing of organic aerosol in the atmosphere and on snow: Effects of SOA and brown
688 carbon, *J. Geophys. Res. Atmos.*, 119, 7453–7476, doi:10.1002/2013JD021186, 2014.

689 Liu, X., Easter, R. C., Ghan, S. J., Zaveri, R., Rasch, P., Shi, X., Lamarque, J.-F.,
690 Gettelman, A., Morrison, H., Vitt, F., Conley, A., Park, S., Neale, R., Hannay, C.,
691 Ekman, A. M. L., Hess, P., Mahowald, N., Collins, W., Iacono, M. J., Bretherton, C.
692 S., Flanner, M. G., and Mitchell, D.: Toward a minimal representation of aerosols in
693 climate models: description and evaluation in the Community Atmosphere Model
694 CAM5, *Geosci. Model Dev.*, 5, 709–739, doi:10.5194/gmd-5-709-2012, 2012.

695 Lu, Z., Streets, D. G., Zhang, Q., and Wang, S.: A novel back-trajectory analysis of
696 the origin of black carbon transported to the Himalayas and Tibetan Plateau during

697 1996–2010, *Geophys. Res. Lett.*, 39, L01809, doi:10.1029/2011GL049903, 2012.

698 Lu, Z., Zhang, Q., and Streets, D. G.: Sulfur dioxide and primary carbonaceous
699 aerosol emissions in China and India, 1996–2010, *Atmos. Chem. Phys.*, 11, 9839–
700 9864, doi:10.5194/acp-11-9839-2011, 2011.

701 Ma, P.-L., Rasch, P. J., Wang, H., Zhang, K., Easter, R. C., Tilmes, S., Fast, J. D., Liu,
702 X., Yoon, J.-H., and Lamarque, J.-F.: The role of circulation features on black carbon
703 transport into the Arctic in the Community Atmosphere Model Version 5 (CAM5), *J.*
704 *Geophys. Res.-Atmos.*, 118, 4657–4669, 2013.

705 Marinoni, A., Cristofanelli, P., Laj, P., Duchi, R., Calzolari, F., Decesari, S., Sellegri,
706 K., Vuillermoz, E., Verza, G. P., Villani, P., and Bonasoni, P.: Aerosol mass and
707 black carbon concentrations, a two year record at NCO-P (5079 m, Southern
708 Himalayas), *Atmos. Chem. Phys.*, 10, 8551–8562, doi:10.5194/acp-10-8551-2010,
709 2010.

710 McConnell, J., Edwards, R. L., Kok, G. L., Flanner, M. G., Zender, C. S., Saltzman, E.
711 S., Banta, J. R., Pasteris, D. R., Carter, M. M., and Kahl, J. D. W.: 20th century
712 industrial black carbon emissions altered Arctic climate forcing, *Science*, 317, 1381–
713 1384, 2007.

714 Ménégoz, M., Krinner, G., Balkanski, Y., Boucher, O., Cozic, A., Lim, S., Ginot, P.,
715 Laj, P., Gallée, H., Wagnon, P., Marinoni, A., and Jacobi, H. W.: Snow cover
716 sensitivity to black carbon deposition in the Himalayas: from atmospheric and ice
717 core measurements to regional climate simulations, *Atmos. Chem. Phys.*, 14, 4237–
718 4249, doi:10.5194/acp-14-4237-2014, 2014.

719 Menon, S., Hansen, J., Nazarenko, L., and Luo, Y.: Climate effects of black carbon
720 aerosols in China and India, *Science*, 297, 2250–2253, 2002.

721 Ming, J., Cachier, H., Xiao, C., Qin, D., Kang, S., Hou, S., and Xu, J.: Black carbon
722 record based on a shallow Himalayan ice core and its climatic implications, *Atmos.*
723 *Chem. Phys.*, 8, 1343–1352, doi:10.5194/acp-8-1343-2008, 2008.

724 Ming, J., Xiao, C., Du, Z., and Yang, X.: An overview of black carbon deposition in
725 High Asia glaciers and its impacts on radiation balance, *Adv. Water Resour.*, 55,
726 80–87, doi:10.1016/j.advwatres.2012.05.015, 2013.

727 Neale, R. B., Chen, C.-C., Gettelman, A., Lauritzen, P. H., Park, S., Williamson, D. L.,
728 Conley, A. J., Garcia, R., Kinnison, D., Lamarque, J.-F., Marsh, D., Mills, M., Smith,
729 A. K., Tilmes, S., Vitt, F., Cameron-Smith, P., Collins, W. D., Iacono, M. J., Easter, R.
730 C., Ghan, S. J., Liu, X., Rasch, P. J., and Taylor, M. A.: Description of the NCAR
731 Community Atmosphere Model (CAM 5.0), NCAR/TN-486+STR, available at:
732 http://www.cesm.ucar.edu/models/cesm1.0/cam/docs/description/cam5_desc.pdf (last

- 733 access: 25 November 2014), 2012.
- 734 Novakov, T., Andreae, M. O., Gabriel, R., Kirchstetter, T. W., Mayol-Bracero, O. L.,
735 and Ramanathan, V.: Origin of carbonaceous aerosols over the tropical Indian Ocean:
736 Biomass burning or fossil fuels, *Geophys. Res. Lett.*, 27, 4061–4064, 2000.
- 737 Novakov, T., Ramanathan, V., Hansen, J. E., Kirchstetter, T. W., Sato, M., Sinton, J.
738 E., and Sathaye, J. A.: Large historical changes of fossil-fuel black carbon aerosols,
739 *Geophys. Res. Lett.*, 30, 1324, doi:10.1029/2002GL016345, 2003.
- 740 Pachauri, R. K.: The future of India's economic growth: the natural resources and
741 energy dimension, *Futures*, 36, 703–713, 2004.
- 742 Qian, Y., Flanner, M. G., Leung, L. R., and Wang, W.: Sensitivity studies on the
743 impacts of Tibetan Plateau snowpack pollution on the Asian hydrological cycle and
744 monsoon climate, *Atmos. Chem. Phys.*, 11, 1929–1948,
745 doi:10.5194/acp-11-1929-2011, 2011.
- 746 Qian, Y., Wang, H., Zhang, R., Flanner, M. G., and Rasch, P. J.: A Sensitivity Study
747 on Modeling Black Carbon in Snow and its Radiative Forcing over the Arctic and
748 Northern China, *Environ. Res. Lett.*, 9(6): Article No.
749 064001, doi:10.1088/1748-9326/9/6/064001, 2014.
- 750 Qian, Y., Yasunari, T. J., Doherty, S. J., Flanner, M. G., Lau, W. K. M., Ming, J.,
751 Wang, H., Wang, M., Warren, S. G., and Zhang, R.: Light-absorbing Particles in
752 Snow and Ice: Measurement and Modeling of Climatic and Hydrological Impact, *Adv.*
753 *Atmos. Sci.*, 32(1), 64–91, doi: 10.1007/s00376-014-0010-0, 2015.
- 754 Rajput, P., Sarin, M., Sharma, D, and Singh, D.: Characteristics and emission budget
755 of carbonaceous species from post-harvest agricultural-waste burning in source region
756 of the Indo-Gangetic Plain, *Tellus B*, 66, 21026, 2014.
- 757 Ram, K., Sarin, M. M., and Hegde, P.: Long-term record of aerosol optical properties
758 and chemical composition from a high-altitude site (Manora Peak) in Central
759 Himalaya, *Atmos. Chem. Phys.*, 10, 11791–11803, doi:10.5194/acp-10-11791-2010,
760 2010.
- 761 Ramanathan, V. and Carmichael, G.: Global and regional climate changes due to
762 black carbon, *Nature Geoscience*, 1, 221–227, 2008.
- 763 Ramanathan, V., Chung, C., Kim, D., Bettge, T., Buja, L., Kiehl, J. T., Washington,
764 W. M., Fu, Q., Sikka, D. R., and Wild, M.: Atmospheric brown clouds: impacts on
765 South Asian climate and hydrological cycle, *Proc. Natl. Acad. Sci. USA*, 102, 5326–
766 5333, 2005.

- 767 Ramanathan, V., Ramana, M. V., Roberts, G., Kim, D., Corrigan, C., Chung, C.,
768 Winker, D.: Warming trends in Asia amplified by brown clouds solar absorption,
769 *Nature*, 448, 575–578, 2007.
- 770 Reddy, M. S. and Venkataraman, C.: Inventory of aerosol and sulphur dioxide
771 emissions from India. Part II – biomass combustion, *Atmos. Environ.*, 36, 699–712,
772 2002.
- 773 Revelle, R.: Energy use in rural India, *Science*, 192, 969–975, 1976.
- 774 Rienecker, M. M., Suarez, M. J., Gelaro, R., Todling, R., Bacmeister, J., Liu, E.,
775 Bosilovich, M. G., Schubert, S. D., Takacs, L., Kim, G.-K., Bloom, S., Chen, J.,
776 Collins, D., Conaty, A., da Silva, A., Gu, W., Joiner, J., Koster, R. D., Lucchesi, R.,
777 and Molod, A.: MERRA – NASA’s Modern-Era Retrospective Analysis for Research
778 and Applications, *J. Clim.*, 24, 3624–3648, 2011.
- 779 Sarka, S., Chokngamwong, R., Cervone, G., Singh, R. P., and Kafatos, M.: Variability
780 of aerosol optical depth and aerosol forcing over India, *Adv. Space Res.*, 37, 2153–
781 2159, 2006.
- 782 Sathaye, J. and Tyler, S.: Transitions in household energy use in urban China, India,
783 the Philippines, Thailand, and Hong Kong, *Annu. Rev. Energ. Environ.*, 16, 295–335,
784 1991.
- 785 Stone, E. A., Lough, G. C., Schauer, J. J., Praveen, P. S., Corrigan, C. E. and
786 Ramanathan, V.: Understanding the origin of black carbon in the atmospheric brown
787 cloud over the Indian Ocean, *J. Geophys. Res.*, 112, D22S23,
788 doi:10.1029/2006JD008118, 2007.
- 789 Streets, D. G. and Waldhoff S. T.: Biofuel use in Asia and acidifying emissions,
790 *Energy*, 23, 1029–1042, 1998.
- 791 Tie, X., Wu, D., and Brasseur, G.: Lung cancer mortality and exposure to atmospheric
792 aerosol particles in Guangzhou, China, *Atmos. Environ.*, 43, 2375–2377, 2009.
- 793 Venkataraman, C., Habib, G., Eiguren-Fernandez, A., Miguel, A. H., and Friedlander,
794 S. K.: Residential biofuels in South Asia: carbonaceous aerosol emissions and climate
795 impacts, *Science*, 307, 1454–1456, 2005.
- 796 Venkataraman, C., Sagar, A. D., Habib, G., Lam, N., and Smith, K. R.: The Indian
797 National Initiative for advanced biomass cook-stoves: the benefits of clean
798 combustion, *Energy Sustain. Dev.*, 14, 63–72, 2010.
- 799 Wang, H., Easter, R. C., Rasch, P. J., Wang, M., Liu, X., Ghan, S. J., Qian, Y., Yoon,
800 J.-H., Ma, P.-L., and Vinoj, V.: Sensitivity of remote aerosol distributions to

801 representation of cloud–aerosol interactions in a global climate model, *Geosci. Model*
802 *Dev.*, 6, 765–782, doi:10.5194/gmd-6-765-2013, 2013.

803 Wang, H., Rasch, P. J., Easter, R. C., Singh, B., Zhang, R., Ma, P. L., Qian, Y., and
804 Beagley, N.: Using an explicit emission tagging method in global modeling of
805 source-receptor relationships for black carbon in the Arctic: Variations, Sources and
806 Transport pathways, *J. Geophys. Res.-Atmos.*, 119, doi:10.1002/2014JD022297,
807 2014.

808 Wang, X., Doherty, S. J., and Huang, J.: Black carbon and other light-absorbing
809 impurities in snow across Northern China, *J. Geophys. Res. Atmos.*, 118, 1471–1492,
810 doi:10.1029/2012JD018291, 2013.

811 Warren, S. G. and Wiscombe, W. J.: A model for the spectral albedo of snow. II:
812 snow containing atmospheric aerosols, *J. Atmos. Sci.*, 37, 2734–2745, 1980.

813 Wiscombe, W. J., and Warren, S. G.: A model for the spectral albedo of snow. I: Pure
814 snow, *J. Atmos. Sci.*, 37, 2712–2733, 1980.

815 Xu, B., Cao, J., Hansen, J., Yao, T., Joswiak, D. R., Wang, N., Wu, G., Wang, M.,
816 Zhao, H., Yang, W., Liu, X., and He, J.: Black soot and the survival of Tibetan
817 glaciers, *Proc. Natl. Acad. Sci. USA*, 106, 22114–22118, 2009a.

818 Xu, B., Wang, M., Joswiak, D. R., Cao, J., Yao, T., Wu, G., Yang, W., and Zhao, H.:
819 Deposition of anthropogenic aerosols in a southeastern Tibetan glacier, *J. Geophys.*
820 *Res.*, 114, D17209, doi:10.1029/2008JD011510, 2009b.

821 Yang, M., Howell, S. G., Zhuang, J., and Huebert, B. J.: Attribution of aerosol light
822 absorption to black carbon, brown carbon, and dust in China—interpretations of
823 atmospheric measurements during EAST-AIRE, *Atmos. Chem. Phys.*, 9, 2035–2050,
824 doi:10.5194/acp-9-2035-2009, 2009.

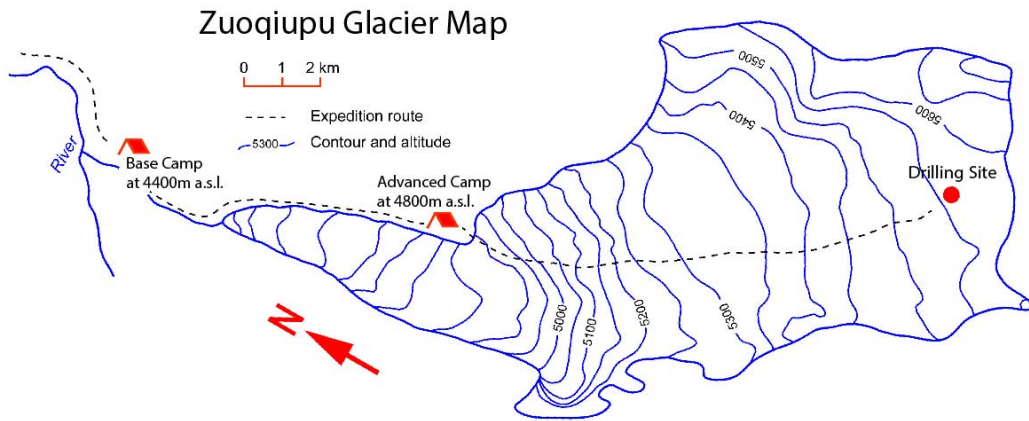
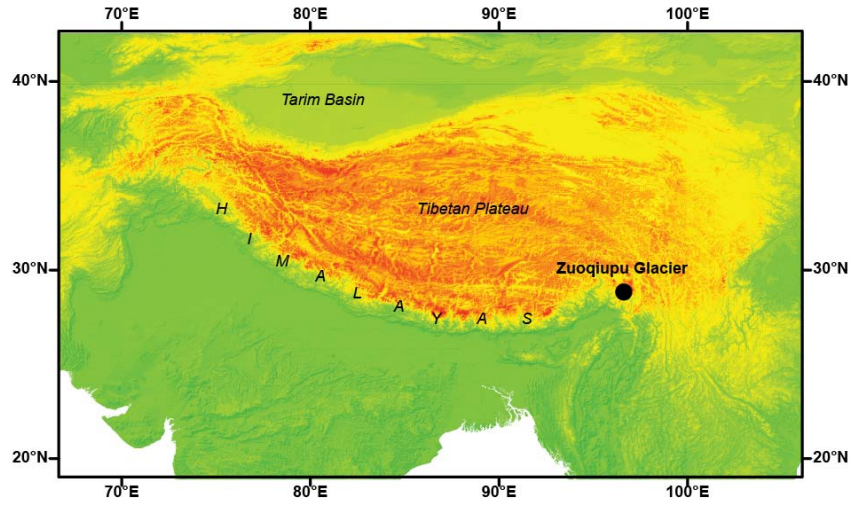
825 Zhao, S., Ming, J., Sun, J., and Xiao, C.: Observation of carbonaceous aerosols during
826 2006–2009 in Nyainqêntanglha Mountains and the implications for glaciers, *Environ.*
827 *Sci. Pollut. Res.*, 20(8), 5827–5838, doi: 10.1007/s11356-013-1548-6, 2013a.

828 Zhao, Z., Cao, J., Shen, Z., Xu, B., Chen, L-W. A., Ho, K., Han, Y., Zhu, C., and Liu,
829 S.: Aerosol particles at a high-altitude site on the Southeast Tibetan Plateau, China:
830 implications for pollution transport from South Asia, *J. Geophys. Res.-Atmos.*, 118,
831 11360–11375, doi:10.1002/jgrd.50599, 2013b.

832 Table 1. Source regions (South Asia, East Asia, Southeast Asia, and Central Asia) and corresponding monthly mean BC emissions (Tg
 833 a⁻¹) and fractional contributions (%) to BC deposition flux at the Zuoqiupu site in monsoon (June-September), non-monsoon
 834 (October-May), and all months during 1996-2005.

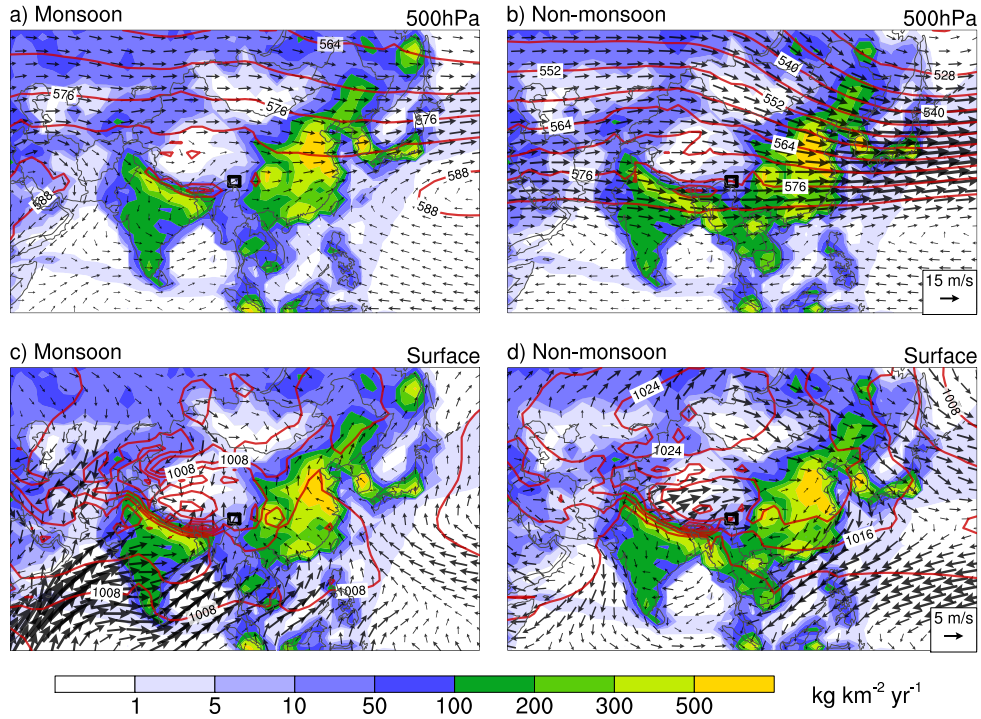
Source Regions	Latitude	Longitude	Monsoon		Non-monsoon		Annual	
			Contribution	Emission	Contribution	Emission	Contribution	Emission
South Asia	5-35°N	50-95°E	38.51	0.65	81.26	0.74	74.48	0.71
East Asia	15-50°N	95-150°E	56.24	1.75	13.91	1.90	20.66	1.85
Southeast Asia	0-15°N	95-130°E	0.05	0.28	0.16	0.33	0.15	0.31
Central Asia	35-50°N	50-95°E	2.62	0.11	0.86	0.09	1.14	0.10

835



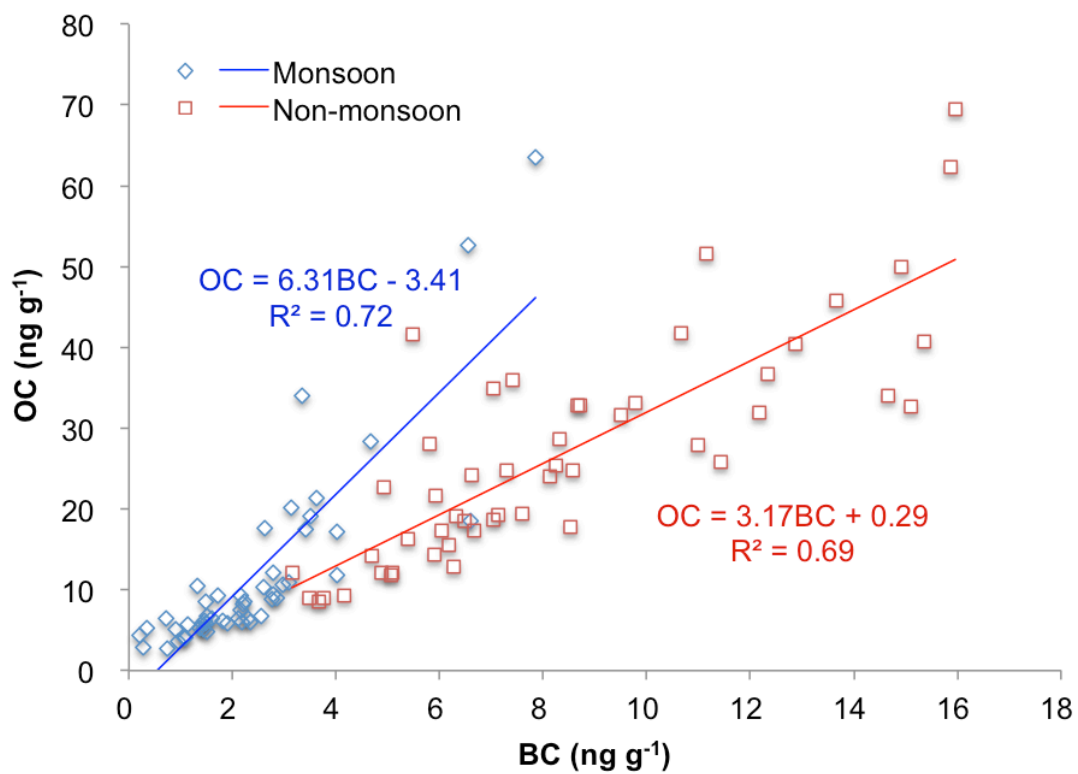
836

837 Figure 1. Site location of Zuoqiupu Glacier (top): black circle represents the location of
 838 Zuoqiupu Glacier, and warm colors indicate high elevations over the Tibetan Plateau.
 839 Detailed elevation contours of the Zuoqiupu Glacier are shown in the bottom panel. Red
 840 circle marks the ice core drill site.



841

842 Figure 2. 10-year (1996-2005) mean wind vectors (denoted by arrows) at 500hPa (a, b)
 843 and the surface (c, d) during summer monsoon (June-September; a, c) and non-monsoon
 844 season (October-May; b, d) from MERRA reanalysis datasets used to drive the CAM5
 845 simulation. 500 hPa Geopotential height (units: 10 m) contours with an interval of 60 m
 846 and mean sea-level pressure (units: hPa) contours with an interval of 4 hPa are
 847 superimposed on panels (a, b) and (c, d), respectively. The background colors show mean
 848 BC emission rates based on the IPCC present-day scenario for the corresponding months.
 849 The small black box marks the model grid-cell in which the ice core drill site resides.

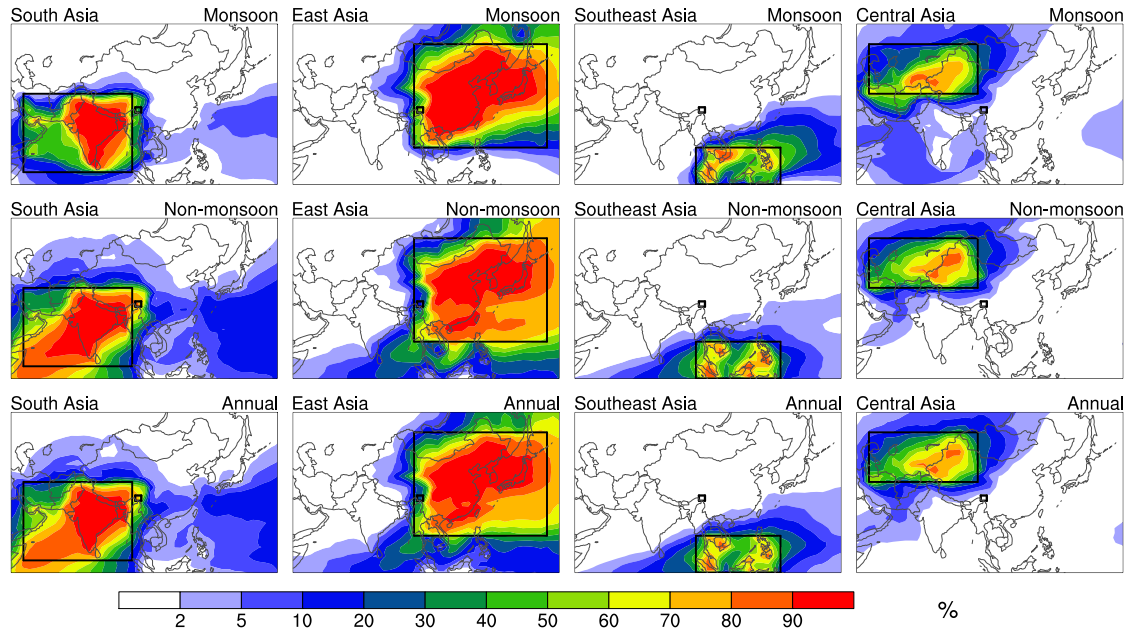


850

851 Figure 3. Scatter plots for yearly monsoon and non-monsoon mean OC and BC
 852 concentrations during 1956-2006, obtained from the ice core measurements, and
 853 corresponding linear regressions.

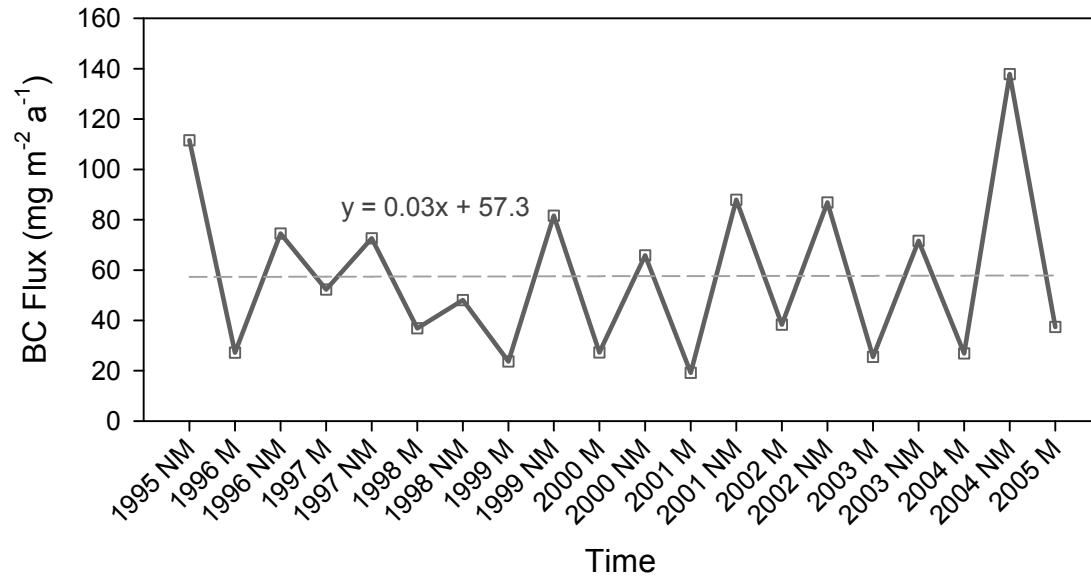
854

855



856 Figure 4. Spatial distributions of fractional contribution from the four source regions
857 (South Asia, East Asia, Southeast Asia, and Central Asia) to monsoon, non-monsoon, and
858 annual mean BC deposition fluxes during 1996-2005. The large black boxes indicate the
859 boundary of source regions, and the small black box marks the model grid-cell where the
860 Zuoqiupu drill site is located. Color in the small black box in each panel corresponds to
861 the fraction contribution to BC deposition at the sampling site. Exact percentage
862 contributions are provided in Table 1.

863



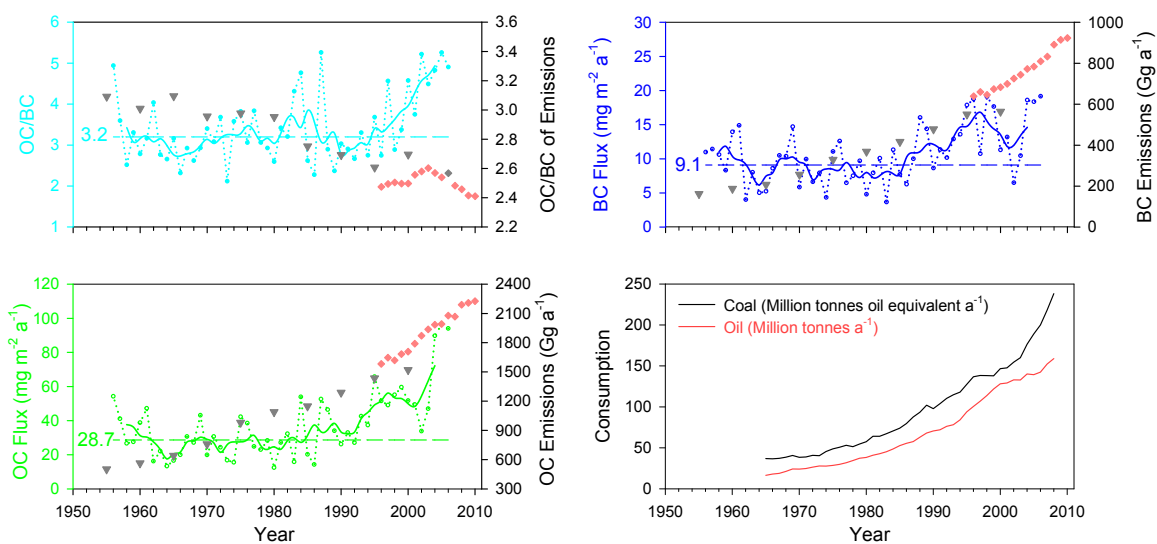
864

865 Figure 5. Seasonal dependence (“NM” for non-monsoon and “M” for monsoon season).

866 of BC deposition flux at the Zuoqiupu site from 1995 to 2005 simulated in CAM5. The

867 dash line represents a linear regression of all data points.

868



869

870 Figure 6 Time series of annual (dotted line with circles) and 5-year averaged (solid line)
 871 OC/BC ratios (top-left), BC (top-right) and OC deposition fluxes (bottom-left) based on
 872 the Zuoqiupu ice core measurements for the time period of 1956-2006. The average
 873 values of OC/BC ratio, BC and OC during 1956-1979 are marked by dashed lines. BC
 874 and OC emissions in South Asia (Bond et al., 2007) and corresponding OC/BC emission
 875 ratios are illustrated with gray triangles, and with red diamonds for emissions in India (Lu
 876 et al., 2011). Coal and oil consumption data are shown in the bottom-right panel (BP
 877 Group, 2009).